

## Diffractive Charm and Dijet Production at H1

---

**Matthias U. Mozer\***

*Physikalisches Institut, Universität Heidelberg, Philosophenweg 12, 69120 Heidelberg,  
Germany*

*E-mail: mozer@physi.uni-heidelberg.de*

The factorization of diffractive  $ep$  cross sections into a (perturbatively accessible) matrix element and a diffractive structure function was proven for the case of DIS by Collins in 1998. Diffractive dijet and open charm production provide a valuable probe to testing factorization and characterize possible mechanisms of factorization breaking.

Measurements of diffractive dijet and open charm production in DIS and photoproduction made with the H1 detector at the HERA accelerator are presented. Diffractive events were identified by a rapidity gap selection. The resulting differential cross sections are compared to QCD calculations in NLO, based on structure functions extracted from inclusive diffraction.

The cross section measurements of diffractive open charm production in DIS and photoproduction agree well with the NLO QCD predictions, supporting factorization. The prediction also describes the dijet data rather well at low momentum fractions  $z_P$  of the diffractive exchange carried by the gluon, where the gluon density is known well from the observed scaling violations of the inclusive diffractive data. A new set of parton densities is obtained by the simultaneous fit to the inclusive diffractive data of previous measurements and the new dijet results. The diffractive dijet cross section in photoproduction is significantly suppressed with respect to the expectations from QCD factorization.

*DIFFRACTION 2006 - International Workshop on Diffraction in High-Energy Physics  
September 5-10 2006  
Adamantas, Milos island, Greece*

---

\*Speaker.

## 1. Introduction

Theoretically it is expected that the cross sections of diffractive deep-inelastic scattering (DIS) factorizes into universal diffractive parton distributions and process dependent hard scattering coefficients [1]. Diffractive parton densities have been determined from DGLAP QCD fits to inclusive diffractive HERA data [2, 3] and have been found to be dominated by the gluon distribution. Diffractive dijet production is directly sensitive to the gluon component of the diffractive exchange and has been shown - for DIS [4] - to be in decent agreement with the QCD fits to the inclusive diffractive data.

While factorization is theoretically well established in diffractive DIS, the appearance of so called resolved photon processes (where the exchanged photon fluctuates into a hadronic state) in diffractive photoproduction complicates the theoretical treatment in this kinematic regime. The additional interactions of this further hadronic system are expected to fill the rapidity gap characteristic of diffraction, leading to a suppression in diffractive photoproduction cross sections compared to the predications of naive factorization [5].

In this paper measurements of diffractive charm and dijet production in DIS and photoproduction are presented; their implications for factorization and the measurement of parton densities is discussed.

## 2. Dijets in DIS

Differential dijet cross sections in diffractive deep inelastic scattering processes at low  $Q^2$  have been measured with the H1 detector using an integrated luminosity of  $51.5 \text{ pb}^{-1}$ . Dijet events are identified using the inclusive  $k_T$  cluster algorithm in the  $\gamma^*$ - $p$  rest frame. The cross sections are given at the level of stable hadrons and correspond to the kinematic range:  $4 \text{ GeV}^2 < Q^2 < 80 \text{ GeV}^2$ ,  $0.1 < y < 0.7$ ,  $x_P < 0.03$ ,  $M_Y < 1.6 \text{ GeV}$ ,  $|t| < 1 \text{ GeV}^2$ ,  $p_{\perp, jet1}^* > 5.5 \text{ GeV}$ ,  $p_{\perp, jet2}^* > 4 \text{ GeV}$  and  $-3 < \eta_{jet}^* < 0$ . Diffractive events are selected by requiring a rapidity gap between the central mass system  $X$  and the proton direction.

Figure 1 shows the differential dijet cross section compared to NLO predictions based on the parton densities from the fit to the inclusive diffractive data [3]. While the prediction based on the H1 2006 DPDF fit A clearly overestimates the cross section, there is reasonable agreement between the data and the H1 2006 DPDF fit B. Nevertheless, significant discrepancies also exist for the H1 2006 DPDF fit B at high  $z_P$ .

The differential dijet cross section in  $z_P$  is used in the fit in 4 bins of the scale variable  $p_{\perp}^{*2} + Q^2$  to constrain the gluon density, where  $p_{\perp}^*$  is the transverse momentum of the hardest jet. These measured cross sections are shown in Figure 2 (left). Additionally the inclusive data sample of a previous H1 analysis [3] is used to constrain the quark density and the gluon density at low momentum fraction. A part of the  $F_2^D$  measurements is shown in Figure 2 (right) together with the final NLO prediction.

The parton densities are parameterized as of momentum fraction  $z$  at a starting scale  $Q_0^2$  as  $A \cdot z^B \cdot (1-z)^C$  and evolved to higher scales by the DGLAP equations in NLO. Here,  $A$ ,  $B$  and  $C$  are free parameters, determined in the fit. Additionally the Regge intercept  $\alpha(0)$  of the pomeron flux factor and the normalization of the sub-leading reggeon exchange enter the fit as free parameters.

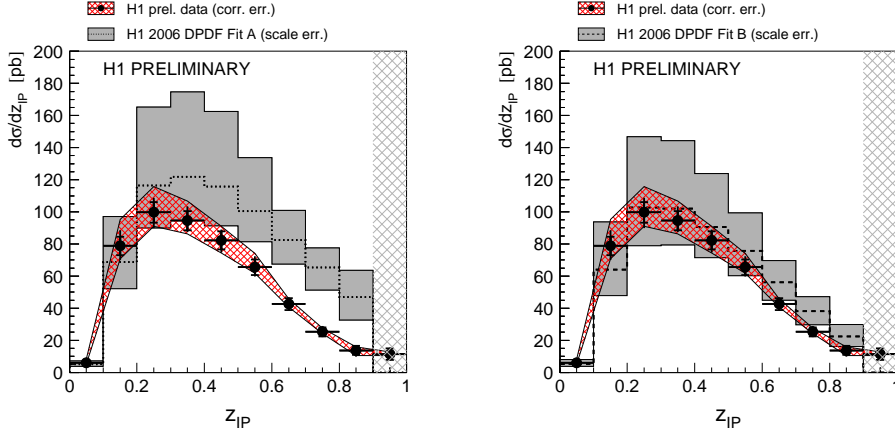


**Figure 1:** Cross section of diffractive dijets differential in  $z_{IP}$  compared to NLO predictions based on the parton-densities from the H1 2006 DPDF fit [3]. The data are shown as black points with the inner and outer error-bar denoting the statistical and uncorrelated systematic uncertainties respectively. The red hatched band indicates the correlated systematic uncertainty. The black line shows the NLO QCD prediction based on the H1 2006 DPDF fit A (left) and H1 2006 DPDF fit B (right) and is surrounded by a grey band indicating the scale uncertainty.

From these parton densities the reduced cross section for inclusive diffractive DIS is computed in NLO as well as the dijet cross section (using the `nlojet++` program).

The fit has a high quality as shown by the overall value  $\chi^2/df = 0.89$  which splits into  $\chi^2/df = 27/36$  for the dijet cross sections and  $\chi^2/df = 169/190$  for  $F_2^D$ . The resulting parton distributions are shown in Figure 3.

As the NLO QCD DGLAP evolution is able to describe both the shape and scaling violations of  $F_2^D$  and the dijet cross sections consistently, we conclude that QCD factorization in DIS is valid in our kinematic region. The data allow for the first time to determine both the diffractive gluon and the singlet quark distribution with good accuracy in the range  $0.1 < z_{IP} < 0.9$ .

### 3. Charm in DIS

Charm cross sections in diffractive DIS were measured by two different methods at H1. In one method the appearance of a charm quark is identified by the reconstruction of a  $D^*$  meson, while the other method identifies tracks not displaced from the primary event vertex to statistically extract the contribution of charm quarks to inclusive diffraction.

The  $D^*$  mesons were identified via the  $D^* \rightarrow D^0 \pi_{slow} \rightarrow K \pi \pi_{slow}$  decay channel.  $D^*$  candidates are restricted to a minimal  $p_t$  of 2 GeV and are required to be well contained within the acceptance of the tracking detectors. The kinematic range is restricted to  $2 < Q^2 < 100 \text{ GeV}^2$ ,  $0.05 < y < 0.7$  and  $x_{IP} < 0.04$ . The final number of  $D^*$ -mesons is obtained by a fit to the  $\Delta M = (M(K, \pi, \pi_{slow}) - M(K, \pi))$ -distribution [6], where  $M(K, \pi, \pi_{slow})$  denotes the invariant mass of the  $K$ ,  $\pi$  and the  $\pi_{slow}$  candidate and  $M(K, \pi)$  denotes the invariant mass of the  $K$  and the  $\pi$  candidate only. The number of  $D^*$  mesons obtained by this fit is  $140 \pm 16$ .

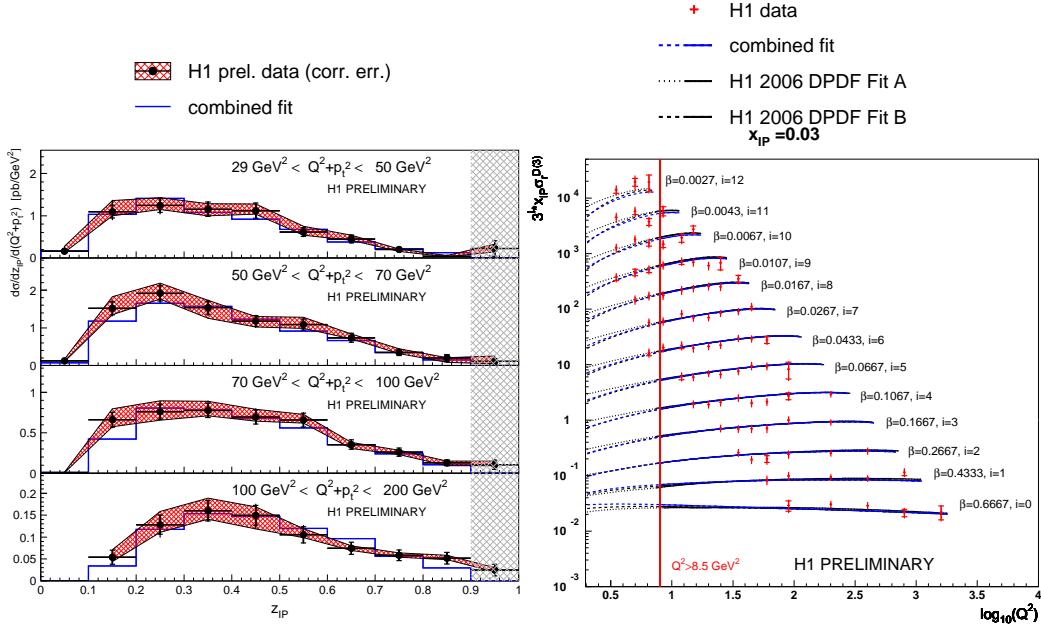


**Figure 2:** left: Cross section of diffractive dijets doubly differential in  $z_P$  and the scale  $\mu = Q^2 + p_\perp^2$ . Uncertainties are denoted as described in Figure 1. The blue line shows the NLO QCD prediction based on the combined fit. right: The  $\beta$  and  $Q^2$  dependence of the diffractive reduced cross section  $\sigma_r^{D(3)}$  multiplied by the pomeron momentum fraction  $x_P$  at  $x_P = 0.03$ . The inner and outer error-bars on the data points represent the statistical and total uncertainties, respectively. The data are compared to the results of the combined fit for  $E_p = 820$  GeV, which is shown as blue lines. The dashed line indicates the prediction in kinematic regions that did not enter into the fit. The two black lines indicate the predictions of the H1 2006 DPDF fit.

Figure 4 shows the resulting cross sections as function of  $z_P$  and  $x_P$ . The cross section are compared to NLO QCD calculations [7] based on a preliminary version of the diffractive parton densities from [3]. The factorization and the renormalization scale are set to  $\sqrt{Q^2 + 4m_c^2}$  and the charm mass is assumed to be  $m_c = 1.5$  GeV. Good agreement between data and prediction is observed, indicating the validity of the factorization approach in diffractive DIS.

The production of open charm in diffraction is also investigated using a largely independent method, which has been used in [8] and [9] to measure the total inclusive charm and beauty cross sections in DIS. This method distinguishes events containing heavy quarks from those containing only light quarks by reconstructing the displacement of tracks from the primary vertex in the transverse plane (impact parameter), caused by the long lifetimes of the charm and beauty flavored hadrons, using the precise spatial information from the central silicon tracker of H1. Due to the low beauty fraction in the diffractive data sample, it is not possible to make a measurement of the beauty cross section and only a measurement of the charm cross section is presented here.

The kinematic variables of the DIS scattering process  $Q^2$  and  $y$  are reconstructed using a method which uses the angle of the hadronic final state in addition to the energy and the polar angle of the scattered positron [3]. The accepted kinematic range in DIS is restricted to  $15 < Q^2 <$

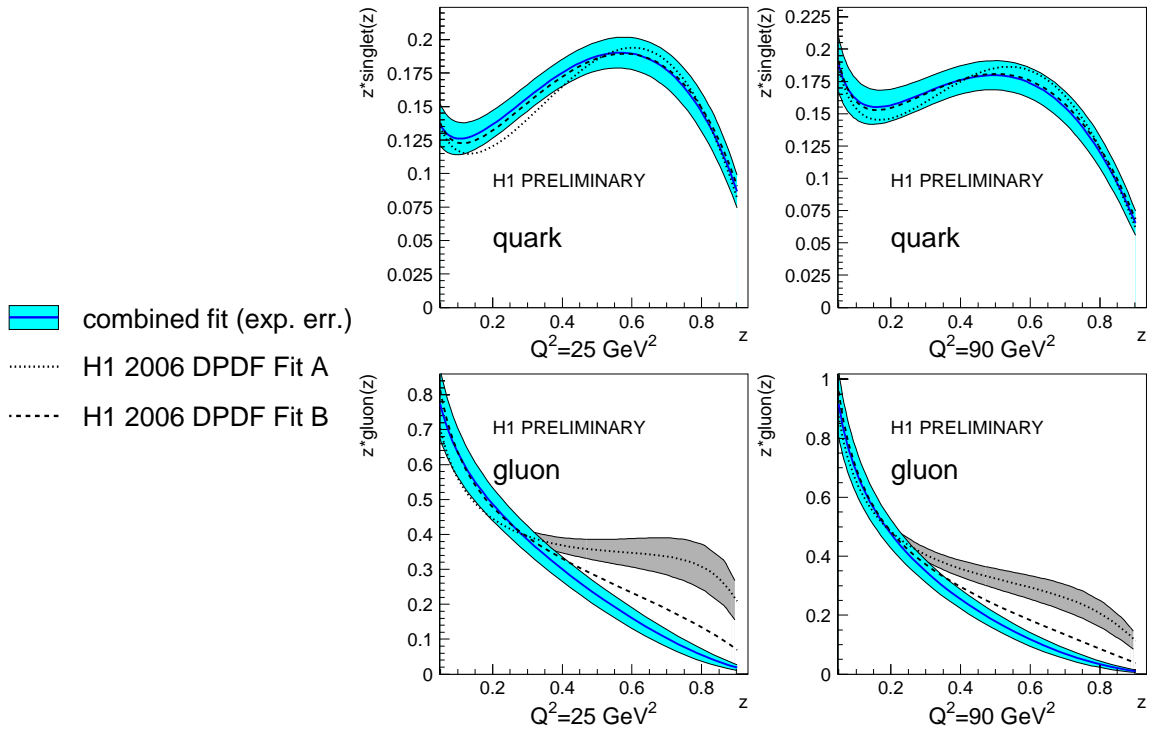


**Figure 3:** The diffractive singlet density (top) and diffractive gluon density (bottom) for two values of the hard scale  $\mu$ :  $25 \text{ GeV}^2$  (left) and  $90 \text{ GeV}^2$  (right). The blue line indicates the combined fit, surrounded by the experimental uncertainty band in light blue. The two dashed lines show the two fit results from [3] for comparison.

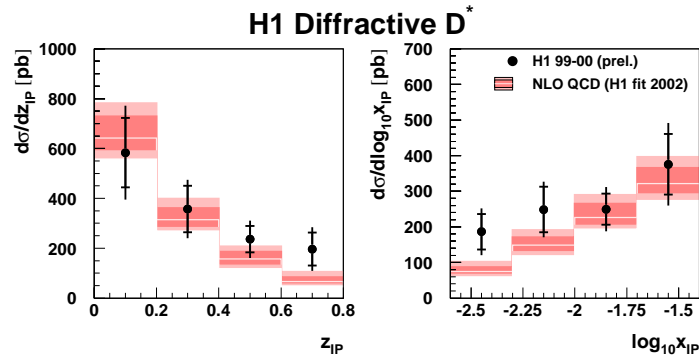


**Figure 4:** The diffractive  $D^*$  cross section in DIS as a function of  $z_{IP}$  (left) and  $x_{IP}$  (right) compared to NLO predictions based on a preliminary version of the parton-densities from the H1 2006 DPDF fit [3]. The data are shown as black points with the inner and outer error-bar denoting the statistical and uncorrelated systematic uncertainties respectively. The white line shows the NLO prediction surrounded by a shaded band indicating the scale uncertainty.

$100 \text{ GeV}^2$  and  $0.07 < y < 0.7$ , where the reduced kinematic range is chosen such that the direction of the struck quark mostly lies within the angular acceptance of the central silicon tracker (CST)

and that the hadronic final state (HFS) has a significant transverse momentum.

After taking into account the effects of detector acceptance, QED radiation, the measured cross sections are corrected to a single point and converted into a measurement of the diffractive open charm reduced cross section  $\tilde{\sigma}_D^{c\bar{c}}$ , defined as:

$$\tilde{\sigma}_D^{c\bar{c}}(x_P, \beta, Q^2) = \frac{d^3 \sigma_D^{c\bar{c}}}{dx_P d\beta dQ^2} \frac{\beta Q^4}{2\pi\alpha^2(1+(1-y)^2)}, \quad (3.1)$$

where  $\alpha$  is the fine structure constant. The reduced cross section is approximately equal to the charm contribution  $F_2^{D(3)c\bar{c}}$  to the diffractive structure function  $F_2^{D(3)}$ .

Figure 5 shows the reduced cross section  $\tilde{\sigma}_D^{c\bar{c}}$  as a function of  $\beta$  for two bins in  $x_P$ . Data points measured with the  $D^*$  and displaced track method from H1 are shown in combination with data points measured with the  $D^*$ -method by the ZEUS collaboration. The data are compared to NLO QCD predictions based on the parton densities from [3]. There is good agreement between the two experiments, the two measurement methods and data and prediction, indicating the validity of factorization.

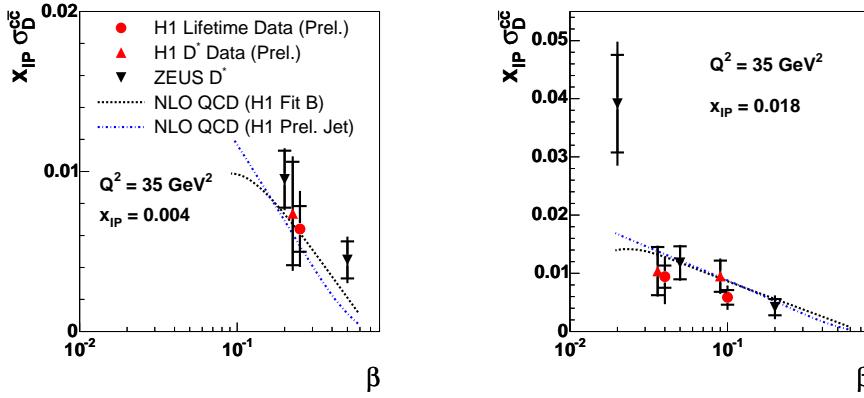


**Figure 5:** Reduced cross section as a function of  $\beta$  in two bins of  $x_P$  compared to NLO QCD prediction based on the parton-densities from the H1 2006 DPDF fit [3] and the combined fit described above.

#### 4. Dijets in Photoproduction

Applying the factorization approach in LO QCD calculations to predict diffractive cross sections for dijet production in  $p\bar{p}$  collisions at the Tevatron leads to an overestimation of the observed rate by approximately one order of magnitude [10]. This discrepancy has been attributed to the presence of the additional beam hadron remnant in  $p\bar{p}$  collisions, which leads to secondary interactions and a breakdown of factorisation. The suppression, often characterized by a ‘rapidity gap survival probability,’ cannot be calculated perturbatively and has been parameterized in various ways (see for example [5]).

The transition from deep-inelastic scattering to hadron-hadron scattering can be studied at HERA in a comparison of scattering processes in DIS and in photoproduction. Processes in which

$Q^2 < 0.01 \text{ GeV}^2$
$165 < W < 242 \text{ GeV}$
inclusive $k_T$ jet algorithm, distance parameter=1
$N_{\text{jet}} \geq 2$
$p_{\perp, \text{jet}1}^* > 5 \text{ GeV}$
$p_{\perp, \text{jet}2}^* > 4 \text{ GeV}$
$-1 < \eta_{\text{jet}(1,2)} < 2$
$x_P < 0.03$

**Table 1:** The kinematic ranges defining the measured dijets cross sections in diffractive photoproduction.

a real photon participates directly in the hard scattering are expected to be similar to the deep-inelastic scattering of highly virtual photons. By contrast, processes in which the photon is first resolved into partons which then initiate the hard scattering resemble hadron-hadron scattering.

The data used in the present analysis were taken in the 1996 and 1997 running periods, in which HERA collided 820 GeV protons with 27.5 GeV positrons, corresponding to an integrated luminosity of  $18 \text{ pb}^{-1}$ . The photoproduction data are collected using a trigger which requires the scattered positron to be measured in the small angle positron detector. Rapidity gap events are selected by requiring an absence of activity in the direction of the outgoing proton. Jets are formed from the hadronic final state using the inclusive  $k_T$  cluster algorithm with a distance parameter of unity in the  $\gamma p$  rest frame. The final jet cross sections are given at the hadron level. The measured distributions are corrected for detector inefficiencies and migrations between measurement intervals during the reconstruction. The kinematic regions in which the cross sections are measured are given in table 1. The kinematic variables  $x_P, M_Y$  and  $t$  are defined on the basis of the largest rapidity gap in the final state hadron distribution which divides the hadrons into the systems  $X$  and  $Y$  (the variables are defined as in [4]).

To obtain NLO cross sections for diffractive dijet photoproduction, the program by Frixione et al. [11] is used. The program is interfaced to the preliminary version of the parton distributions obtained in [3]. For the comparison with the measured hadron level jet cross sections, the calculated NLO parton jet cross sections were corrected for the effects of hadronisation using the RAPGAP Monte Carlo generator with Lund string fragmentation.

Figure 6 shows the measured cross section of diffractive dijet photoproduction compared to QCD calculations assuming factorization. The QCD calculations are higher by a factor  $\approx 2$  compared with the experimental results, showing the breakdown of factorization in diffractive photoproduction. The factorization breaking also occurs for all values of the momentum fraction entering the hard interaction from the photon side ( $x_\gamma$ ), contrary to the predictions of [5].

### 5. Charm in Photoproduction

The analysis of charm in diffractive photoproduction closely follows the analysis of diffractive  $D^*$  production in DIS discussed above. Instead of detecting the scattered lepton in the backward calorimeter, it is detected in a low angle tagging detector, which restricts the accessible kinematics

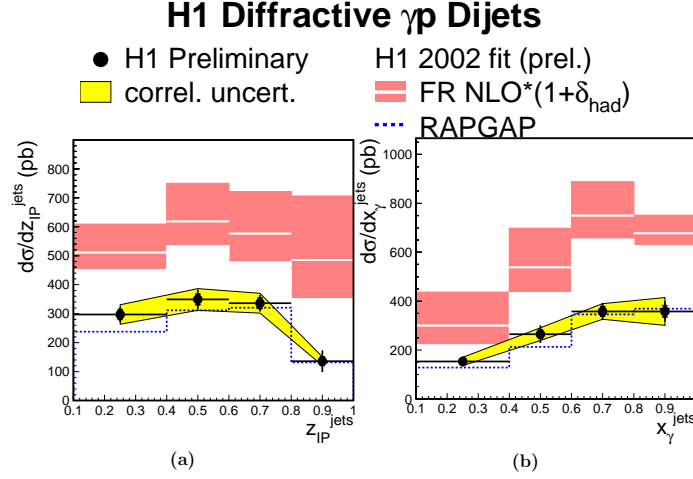


**Figure 6:** The diffractive dijet cross section in photoproduction as a function of  $z_{IP}$  (left) and  $x_\gamma$  (right) compared to NLO predictions based on a preliminary version of the parton-densities from the H1 2006 DPDF fit [3]. The data are shown as black points with the inner and outer error-bar denoting the statistical and uncorrelated systematic uncertainties respectively. The white line shows the NLO prediction surrounded by a shaded and indication the scale uncertainty.

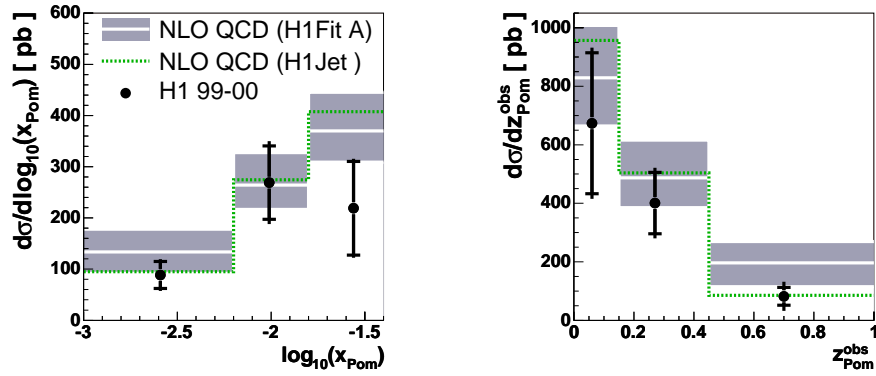
to  $Q^2 < 0.01$  and  $0.3 < y < 0.65$ .  $x_P$  is restricted to the range below 0.04. The reconstruction of the  $D^*$  meson itself is identical to the analysis mentioned above.

Figure 7 shows the resulting cross sections as function of  $z_{IP}$  and  $x_P$ . The cross sections are compared to NLO QCD calculations [7] based on parton densities from [3] and the combined fit discussed above. The factorization and the renormalization scale are set to  $\sqrt{p_t^2 + 4m_c^2}$  and the charm mass is assumed to be  $m_c = 1.5$  GeV. Fair agreement between data and prediction is observed, indicating that factorization holds for diffractive charm production even in photoproduction. This evidence for factorization in diffractive photoproduction applies only to the direct contribution, as the resolved contribution in diffractive open charm production is kinematically suppressed. However, the statistical uncertainties of the measurement are rather large, precluding strong conclusions.

## 6. Conclusion

Measurements of diffractive dijet and open charm production in DIS and photoproduction were presented. In DIS the results are consistent with QCD factorization. The dijet data sample was used in combination with a measurement of inclusive diffraction to extract diffractive parton densities with an NLO DGLAP fit.

In photoproduction, the measurement of diffractive open charm production is consistent with QCD factorization. The measurements of diffractive dijet cross sections in photoproduction, however, lie significantly lower than the NLO QCD predictions based on factorization. Notably, the discrepancy does not depend on  $x_\gamma$ .



**Figure 7:** The diffractive  $D^*$  cross section in photoproduction as a function of  $z_P$  (left) and  $x_P$  (right) compared to NLO predictions based on the parton-densities from the H1 2006 DPDF fit [3] and the combined fit discussed above. The data are shown as black points with the inner and outer error-bar denoting the statistical and uncorrelated systematic uncertainties respectively. The white line shows the NLO prediction for the H1 2006 DPDF fit A surrounded by a shaded band indicating the scale uncertainty. The dashed line indicates the prediction using the combined fit.

## References

- [1] J. Collins, Phys. Rev. **D57** (1998) 3051 and erratum-ibid. **D61** (2000) 019902.
- [2] C. Adloff *et al.* [H1 Collaboration], Z. Phys. **C76** (1997) 613.
- [3] DESY-06-049, [arXiv:hep-ex/0606004].
- [4] H1prelim-04-113.
- [5] A. Kaidalov, V. Khoze, A. Martin, M. Ryskin, Phys. Lett. **B567** (2003) 61.
- [6] G. J. Feldman *et al.*, Phys. Rev. Lett. **38** (1977) 1313.
- [7] B. W. Harris, J. Smith, Nucl. Phys. **B 452** (1995) 109, [arXiv:hep-ph/9503484];  
L. Alvero, J. C. Collins, J. J. Whitmore, PSU-HT **200** (1998) 13, [arXiv:hep-ph/9806340].
- [8] A. Aktas *et al.* [H1 Collaboration], Eur. Phys. J. C **40** (2005) 349 [arXiv:hep-ex/0411046].
- [9] A. Aktas *et al.* [H1 Collaboration], Eur. Phys. J. C **45** (2006) 23 [arXiv:hep-ex/0507081].
- [10] T. Affolder *et al.*, [CDF Collaboration], Phys. Rev. Lett. **84** (2000) 5043.
- [11] S. Frixione, Z. Kunszt and A. Signer, Nucl. Phys. **B467** (1996) 399;  
S. Frixione, Nucl. Phys. **B507** (1997) 295.